Simple refinements of Brillouin zone integration

2000 J. Phys.: Condens. Matter 12 549

(http://iopscience.iop.org/0953-8984/12/5/303)

J. Phys.: Condens. Matter **12** (2000) 549–558. Printed in the UK PII: S0953-8984(00)07878-4

Simple refinements of Brillouin zone integration

J A O Bruno†, N L Allan‡ and T H K Barron‡

† Departamento de Química Inorgánica, Analítica y Química Física, Facultad de Ciencias Exactas y Naturales, Universidad de Buenos Aires, Pabellón 2, Ciudad Universitaria, 1428 Buenos Aires, Argentina

‡ School of Chemistry, University of Bristol, Cantock's Close, Bristol BS8 1TS, UK

Received 16 September 1999

Abstract. Calculations of thermodynamic properties of crystals by means of quasi-harmonic lattice dynamics require numerical integrations over the Brillouin zone, using successively finer grids to achieve convergence to the required precision; but for complex crystals convergence may be uneconomically slow. A model for orthorhombic polyethylene is used to show how convergence may be improved (1) at low temperatures by taking successively finer grids close to the origin of reciprocal space, and (2) at all temperatures by using a three-dimensional Simpson's rule.

1. Introduction

In the quasi-harmonic approximation, the Helmholtz free energy F is expressed as an integral over the first Brillouin zone (or an equivalent region) in reciprocal $\boldsymbol{q}$-space, where $\boldsymbol{q}$ is a phonon wave-vector (e.g. Taylor *et al* 1997, Barron and White 1999):

$$F = \frac{V}{(2\pi)^3}\int_{\mathrm{FBZ}} \mathrm{d}\boldsymbol{q} \sum_s f[\hbar\omega_{\boldsymbol{q}s}(kT)^{-1}]. \tag{1}$$

Here V is the volume, k is Boltzmann's constant, the sum over s is taken over all the vibrational modes $\boldsymbol{q}s$ with wave-vector $\boldsymbol{q}$, and f is the function

$$f(x) = kT[\tfrac{1}{2}x + \ln(1 - \mathrm{e}^{-x})]. \tag{2}$$

For comparison with experiment, we require not only the free energy but also other properties such as the heat capacity and thermal expansion, which may often be measured to accuracies of 1% or better. At least at low temperatures, these can be obtained more precisely by integrating explicit analytic expressions over the FBZ rather than by differentiating the calculated free energy numerically. Thus the constant-volume heat capacity is given by

$$C_V = \frac{V}{(2\pi)^3}\int_{\mathrm{FBZ}} \mathrm{d}\boldsymbol{q} \sum_s c[\hbar\omega_{\boldsymbol{q}s}(kT)^{-1}] \tag{3}$$

where c is the function

$$c(x) = kx^2[(\mathrm{e}^x - 1)(1 - \mathrm{e}^{-x})]^{-1}. \tag{4}$$

The integration is often carried out using uniform grids in $\boldsymbol{q}$-space§. The frequencies are obtained by diagonalizing the dynamical matrix for each $\boldsymbol{q}$, and their strain derivatives (required for essentially anharmonic properties such as the thermal expansion) from derivatives

§ Spectral properties such as the frequency distribution require special treatment (Gilat 1976).

0953-8984/00/050549+10$30.00

of this matrix by means of first-order perturbation theory (e.g. Wallace 1972, Barron 1998). This can be achieved easily for a crystal structure with only a few atoms per primitive cell and consequently a small dynamical matrix, but it becomes rapidly more time consuming for larger dynamical matrices, especially when there are long-range Coulomb forces between atoms. It may then be very expensive to use uniform integration grids fine enough to give the required accuracy, particularly at low temperatures. More efficient methods are needed.

In this paper we describe two techniques we have found useful in recent work on a model for the highly anisotropic thermal expansion of crystalline polyethylene at low temperatures (Bruno *et al* 1998). The orthorhombic unit cell of polyethylene is of moderate size, containing twelve atoms which belong to two conformationally equivalent chains; the calculation of the phonon frequencies then requires the diagonalization of a 36×36 dynamical matrix at each point $\boldsymbol{q}$ of the integration grid. In calculations on this crystal, Lacks and Rutledge (1994) used coarse integration grids containing either 32 or 108 independent $\boldsymbol{q}$-points in the FBZ, which gave F to within 0.01 kJ mol^{-1}; to obtain the thermal expansion, F was then minimized numerically at different temperatures with respect to the lattice parameters. This worked well, but was insufficiently precise to give detailed behaviour at low temperatures. In contrast, the calculations described in the present paper were directed primarily at the understanding of low-temperature behaviour. The model uses the short-range VFF2 molecular mechanics force field described previously by Bruno *et al* (1998). The crystal is sufficiently complex to give rise to difficulties in the zone integration, but small enough for these to be resolved relatively easily, thus providing an efficient means of examining the effectiveness of different methods of Brillouin zone integration.

A very common method is that described by Monkhorst and Pack (1976), employing a grid of equally spaced wave-vectors none of which lie along the boundary of the Brillouin zone. Reciprocal space is divided into cells similar in shape to the reciprocal-lattice unit cell but smaller in linear dimensions by a factor $1/m$, where m defines the inverse mesh size. The grid comprises the centres of the cells, as illustrated for a two-dimensional lattice in figure 1. These are 'special points', in the sense that using them ensures that low Fourier components of a periodic function in $\boldsymbol{q}$-space are integrated correctly (Chadi and Cohen 1973, Cunningham 1974, Dal Corso 1996).

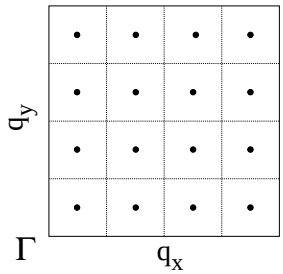

Figure 1. A uniform grid comprised of cell centres, in the positive quadrant of the FBZ of a two-dimensional rectangular lattice.

But a grid of this type can only sample points close to the boundary of the integration region, including those near to the Γ point, when a very fine mesh is used. For this reason the method is insensitive at low temperatures, an important range where experimental data on heat capacity and thermal expansion are often available. In the next section we discuss how the method can be adapted to sample points close to the Γ point more efficiently.

2. Low temperatures

The full line in figure 2(a) shows the variation with mesh size $(1/m)$ of the coefficient of thermal expansion α along the a-axis of crystalline polyethylene at 0.4 K.

At low frequencies the vibrational frequency distribution of a crystal is given by the asymptotically convergent series

$$g(\omega) = a\omega^2 + b\omega^4 + c\omega^6 + \cdots \tag{5}$$

leading to a vibrational heat capacity at low temperatures of the form

$$C_{vib} = AT^3 + BT^5 + CT^7 + \cdots . \tag{6}$$

The first terms in these series can be derived from the elastic moduli of the crystal, by generalizing Debye's well known isotropic theory to elastically anisotropic materials. The further terms arise because of dispersion; in other words, because the dependence of phonon frequencies on wavenumber is not linear. Similar series exist for coefficients of thermal expansion.

Departures from the Debye T^3-limit due to dispersion are seen clearly in plots of C_{vib}/T^3 against T^2, and also in plots of the Debye equivalent temperature $\Theta^C(T)$ against T; see, e.g., Barron and White (1999). They become appreciable at surprisingly low temperatures, even for such simple crystal structures as cubic close packed, diamond or rock-salt. Typically deviations are of the order of 1% when $T \approx \Theta/100$, and may rapidly increase with T thereafter; e.g., for grey tin Θ^C has fallen by 25% when $T \approx 6$ K. With more complex structures, including orthorhombic polyethylene, the combination of weak and strong interatomic forces within the same crystal can lead to striking variations of behaviour, especially in the thermal expansion of anisotropic materials; in α-quartz, for example, where the torsional forces are weak, the expansion coefficient along the trigonal axis becomes negative below 12 K, and T^3-behaviour is not found until lower temperatures are reached. Thus thermodynamic properties at low temperatures cannot be obtained by extrapolation from higher temperatures; rather, they give additional information about the solid. Theoretical models are therefore severely tested by their ability to reproduce the variation of heat capacity and thermal expansion at low temperatures, together of course with other experimental data. To apply this test we need precise integration over the FBZ near the Γ point.

Fortunately, in one respect the calculation of thermodynamic properties at low temperatures is greatly simplified compared to that at higher temperatures. Because the total thermal expansion is usually very small, we do not have to optimize the equilibrium geometry at each temperature: negligible error is incurred by taking the equilibrium geometry at $T = 0$ over the whole low-temperature range. Computation of thermodynamic properties at different temperatures can therefore be carried out simultaneously, and at each point of the integration grid the frequencies and their strain derivatives need be found only once.

The crystal symmetry enables us to restrict the integration to the positive octant, and so $m^3/8$ independent wave-vectors are included in each integration. The failure of all the mesh sizes to give adequate results at low temperatures is evident; for example, even for $m = 32$ (4096 points) the calculated value of α_a is effectively zero, since none of the sampled modes are excited appreciably at 0.4 K. The difference between the values obtained for $m = 48$ (13 824 points) and $m = 64$ (32 768 points) indicate that we are still far from convergence with increasing m, and hence that a much finer mesh would be needed for adequate sampling of modes close to the Γ point. At 1 K the grid with $m = 8$ (64 points) still samples no active modes, and the value of α_a changes by about 17% from $m = 48$ to $m = 64$, as shown by the full line in figure 2(b). Only for temperatures above 5 K is adequate convergence (error less than 1%) achieved for $m = 32$ (figure 2(c): full line).

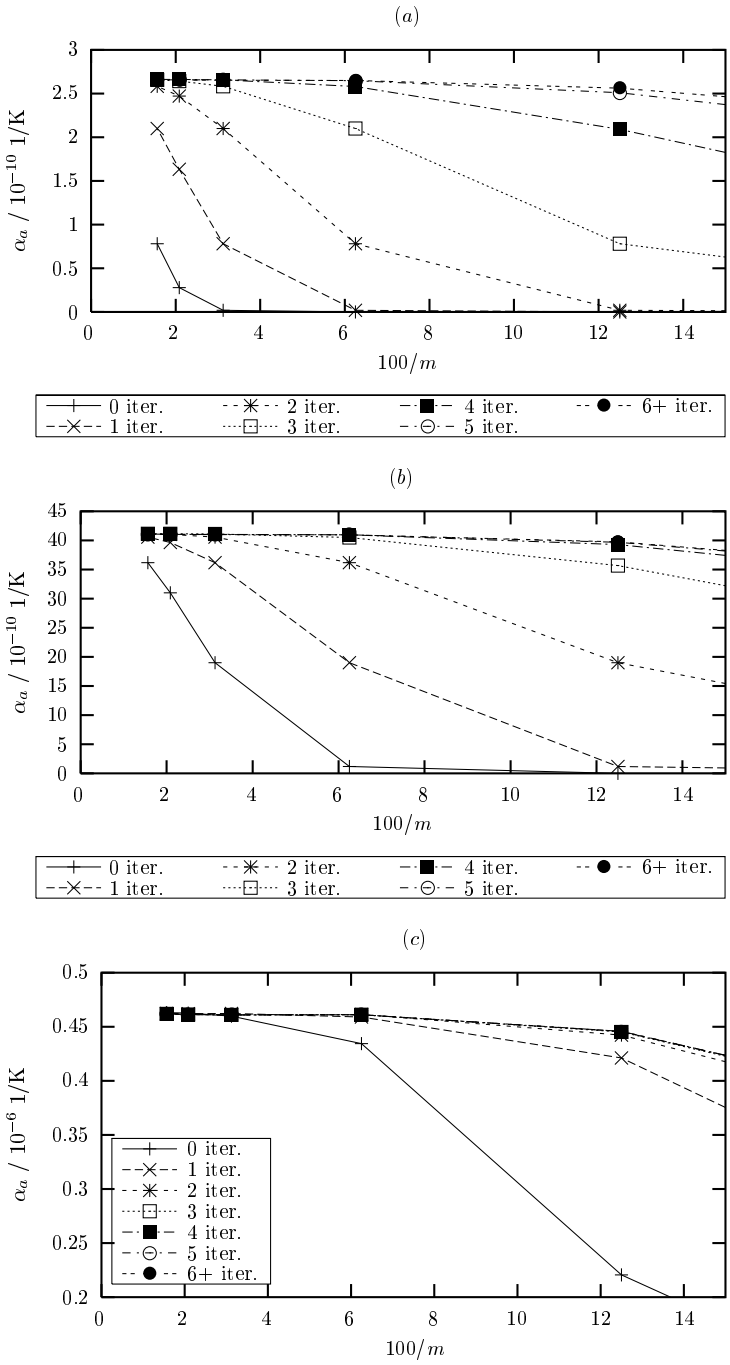

Figure 2. Calculated thermal expansion coefficients for the a-direction (α_a) of crystalline orthorhombic polyethylene as a function of mesh size $1/m$: (a) at 0.4 K; (b) at 1 K; (c) at 5 K. Full lines are the results from a uniform grid of cell centres as described in the text. Others use finer meshes in inner regions of the FBZ, with the number of iterations indicated. On the right of the figure the lines are directed towards points given by $m = 4$.

Thus it is clear from figure 2 that the uniform grid of cell centres is not well suited to the evaluation of thermal properties at low temperatures.

Since the contribution to these from outer parts of the zone is negligible a very fine grid over the entire Brillouin zone would be grossly wasteful. Rather, we need a systematic method of progressively increasing the density of points as the Γ point is approached. To this end we adapt an iteration method applied previously to a model for α-quartz (Barron and Pasternak 1987). In the first step the integration over the inner region with linear dimension half that of the full zone is recalculated with a finer grid employing the same number of points as that used originally for the full zone. In the next iteration this inner region is itself treated in a similar way, and so on until satisfactory convergence is achieved. Usually the linear dimensions of successive inner regions are halved each time, but other factors are possible; for example, a factor of one-third was used for α-quartz. Figure 3 illustrates the procedure (in two dimensions) for meshes $m = 2, 4, 8$.

Figure 2 shows results obtained using this iterative approach for α_a at three different low temperatures. For mesh size $1/m$, a total of $(n + 1)m^3/8$ wave-vectors are sampled after n iterations. Convergence with respect to increasing m is much improved compared to that for a uniform mesh of cell centres ($n = 0$). Different symbols are used to show how the convergence with m changes as the number of iterations n is increased ($n = 1, \ldots, 6$). In general terms, the coarser the mesh and the lower the temperature, the more iterations needed. At 0.4 K satisfactory convergence is achieved after six iterations for mesh $m = 8$, and after only three for mesh $m = 64$. At 1 K, for mesh $m = 8$ four iterations are required, and just one iteration is needed for mesh $m = 64$. At 5 K, only two iterations are needed for mesh $m = 8$.

As $T \rightarrow 0$ the Debye limit is approached, where the heat capacity and thermal expansion vary as T^3. The coefficients of T^3 can also be derived from the elastic stiffnesses and their strain dependence; this involves integration over all directions of propagation of elastic waves, i.e. over all directions in $\boldsymbol{q}$-space emanating from the Γ point (e.g. Barron and White 1999, section 2.9). Figures 3(a) and 3(b) show how the directions of points sampled in $\boldsymbol{q}$-space depend only on the inverse mesh size m and are unaffected by the iteration procedure. A coarse mesh of low m gives points along only a few directions in $\boldsymbol{q}$-space and can be expected to give only crude estimates of the T^3-coefficients, even after the iterative procedure has been used.

3. Using a three-dimensional Simpson's rule

Even with the iterative method described above, convergence with increasing m can sometimes still be very slow. Figure 4 is analogous to figure 2(c), but instead of α_a plots α_b, the coefficient of thermal expansion along the b-axis, again at 5.0 K as a function of mesh size. Although the iterative procedure for each m has fully converged by $n = 4$, the limiting value for large m has not been reached even for $m = 64$.

Consideration of the physics of the model suggests that the slow convergence may be due to the rapid change in the nature of vibrational modes as the plane $q_z = 0$ is approached in reciprocal space. When $q_z = 0$, distances between second neighbours in the carbon skeletons remain unaltered, and so the lower-frequency modes need not involve the strong forces maintaining the C–C distances and the C–C–C angles; but away from the q_z-plane these forces are necessarily brought into play. Now the Monkhorst–Pack grids do not sample any points on this plane. But we can include points for which $q_z = 0$ if we transpose each grid so that it now samples the corners of cells rather than the cell centres. Since rapid variation of integrands near $q_z = 0$ implies significant amplitudes of some high Fourier components, it need not worry us that these are not 'special points'. Integration with this grid of cell

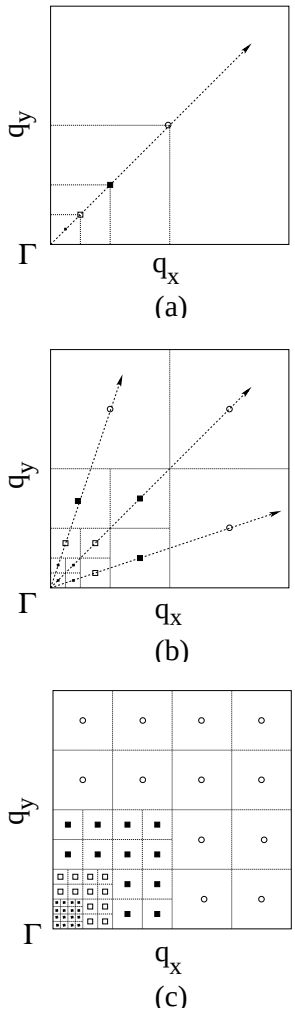

Figure 3. Two-dimensional grids illustrating the iterative procedure that is described in the text; (a) mesh $m = 2$, (b) mesh $m = 4$, (c) mesh $m = 8$. The points used in the first quadrant for up to three iterations are shown. The symbol used to denote each point specifies its relative weighting factor in the integration. The weighting factor of the black squares is 1/4 that of the open circles; that of the open squares is 1/4 that of the black squares; and that of the black circles is 1/4 that of the open squares. In three dimensions successive weighting factors are reduced by 1/8 instead of 1/4.

corners does indeed raise additional problems, but these are solved by using the following strategies.

(i) The grid includes points on the boundary of the integration region. This not only means that the number of independent points is increased from $(m/2)^3$ to $[(m/2) + 1]^3$, but also that points on the boundary have their weights reduced by a half for each face of the integration region in which they occur; thus for points on edges the reduction factor is a quarter and for points on corners of the integration region the factor is one eighth.

(ii) The grid includes the Γ point, for which the acoustic Grüneisen parameters are indeterminate. The Γ point is therefore omitted from both numerator and denominator

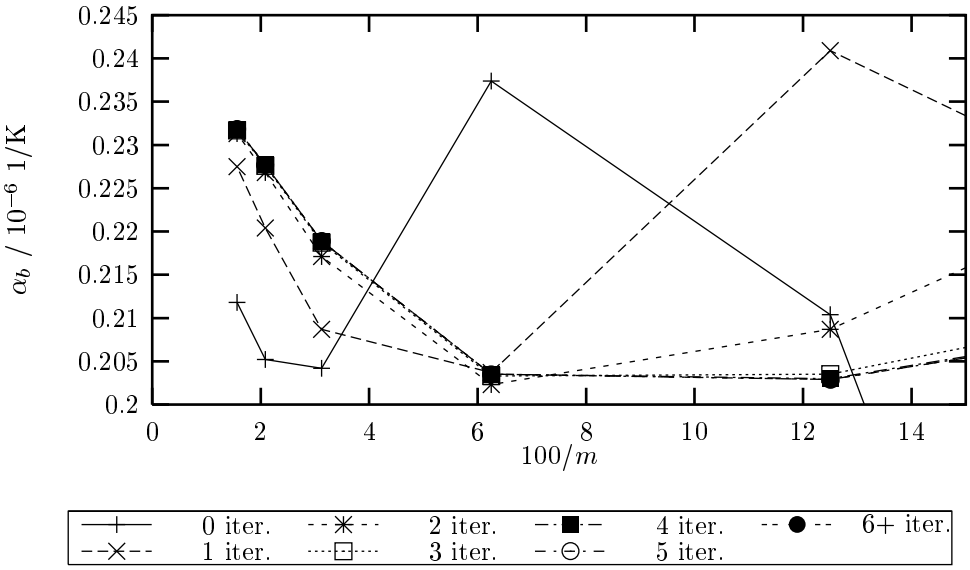

Figure 4. Calculated value of α_b for crystalline orthorhombic polyethylene at 5 K as a function of mesh size. The full line shows results obtained using uniform grids of cell centres. Others use finer meshes in inner regions of the FBZ, with the number of iterations indicated.

when taking averages over the integration region (Barron and Gibbons 1974). This is a potentially serious source of error for coarse meshes, but is eliminated when the iterative technique is used and the weight of the Γ point thus becomes negligible.

(iii) Care is needed in the iterative procedure with the weights of points on the boundary separating the inner and outer region, since they contribute to both regions. A simple way of determining the weights of these in each region is to take Wigner–Seitz cells about each grid point; the weight of the point is determined by the volume of the part of the Wigner–Seitz cell that falls within the region.

Figure 5(a) shows values for both cell-centre and cell-corner grids of α_b at 5 K, calculated with six inner-region iterations, as functions of mesh size. It is clear that the errors produced by the centre grid are overcorrected by using the corner grid. We have therefore adopted a device previously used by Barron and Gibbons (1974) for a rhombohedral lattice, and employed a three-dimensional analogue of Simpson's rule. In one dimension, the basis of Simpson's rule is that the integral of a quadratic function over any interval is obtained correctly from its value at the centre of the interval and its values at both extremities, provided that the value at the centre is given a weight four times that at each of the extreme points. Similarly, in three dimensions it is easy to show that the integral of a quadratic function over a cell with parallel faces is obtained correctly from its value at the cell centre and its values at the cell corners, provided that the centre value is given a weight sixteen times that at each corner†. But each cell centre belongs to one cell only, whereas each corner point in the interior of the integration region is shared by eight cells. Consequently, applying a three-dimensional Simpson's rule is equivalent to combining the integral obtained from the centre grid and that obtained from the corner grid of the same mesh size with respective weighting $\frac{2}{3}$ and $\frac{1}{3}$; the integration would then be exact if the integrand were quadratic in each grid cell.

† In two dimensions the weight at the centre would be eight times that at each of the corners.

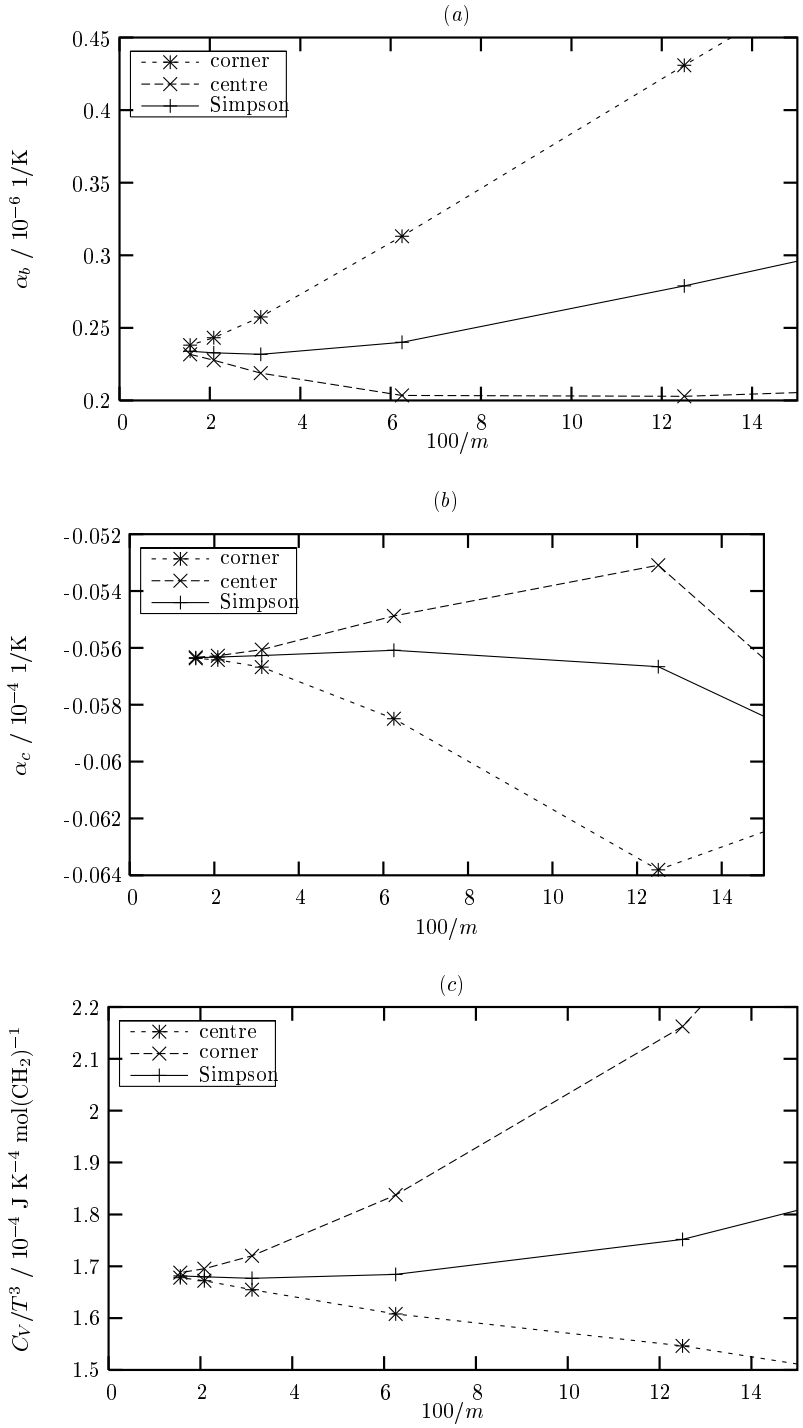

Figure 5. Calculated thermodynamic properties (after six iterations of inner regions) as a function of mesh size for centre grid ($\times$) and corner grid ($*$), compared with those obtained by applying Simpson's rule (full line). (a) α_b at 5 K, (b) α_c at 100 K, (c) C_V/T^3 at 0.4 K.

This simple method works well, and gave the degree of convergence that we required. In figure 5(a) the full line shows the value obtained by combining the two grids in this way. Immediately evident is the improved convergence of the full line over the use of either corner or centre grids alone. Convergence to within 1% is achieved for mesh $m = 16$.

Simpson's rule is useful at all temperatures. In figure 5(b) calculated values of α_c at 100 K (negative, in agreement with experiment) are plotted against mesh size, and again the combination of the two grids gives more rapid convergence than that given by either of the separate grids.

The method can also be used for other thermodynamic quantities, such as the heat capacity. In figure 5(c) the variation with mesh size of C_V/T^3 at $T = 0.4$ K is seen to converge to within 1% with mesh $m = 16$. Plots of C_V/T^3 against T^2 show that at this temperature deviations from Debye limiting behaviour are small, and so this result is suitable for comparison with theoretical or experimental elastic behaviour.

4. Conclusions

For many applications a uniform integration grid formed by sub-dividing the reciprocal-lattice cells and taking the centres of the sub-cells works well; it avoids singularities at $\boldsymbol{q} = 0$, and accuracy can be tested by taking finer grids. For some symmetries other regular grids may also be appropriate, as for trigonal crystals (Barron and Pasternak 1987). Further refinements are needed only when achieving convergence becomes computationally expensive.

Over the whole low-temperature range, heat capacity, thermal expansion, and related properties can be calculated at the $T = 0$ geometry, without the need to optimize the structure at each temperature. But at low temperatures it is essential to refine the integration grid progressively in the neighbourhood of the zone centre $\boldsymbol{q} = 0$. This can be done by an iterative procedure in which progressively finer meshes are taken in inner regions around the zone centre, each iteration taking about the same CPU time as for the original mesh used at high temperatures. The number of iterations needed depends upon the fineness of the original mesh, the lowest temperatures used, and the precision required. No further knowledge is gained in proceeding to lower temperatures once the limiting T^3-behaviour is reached.

Faster convergence with respect to the total number of grid points used may sometimes be obtained by taking also the corner points of grid cells, and applying a three-dimensional Simpson's rule. This is particularly useful when the integrand changes rapidly near boundaries of the integration region.

Acknowledgments

Computational resources for this work were funded by EPSRC grants GR/L31340 and GR/M34799. JAOB's contribution was made possible by means of Grant UBACyT JX-14 from the University of Buenos Aires.

References

Barron T H K 1998 *Thermal Expansion of Solids (CINDAS Data Series on Material Properties vol I-4)* ed C Y Ho (Materials Park, OH: ASM International) ch 1

Barron T H K and Gibbons T G 1974 *J. Phys. C: Solid State Phys.* **7** 3287

Barron T H K and Pasternak A 1987 *J. Phys. C: Solid State Phys.* **20** 215

Barron T H K and White G K 1999 *Heat Capacity and Thermal Expansion at Low Temperatures* (New York: Kluwer/Plenum)

Bruno J A O, Allan N L, Barron T H K and Turner A D 1998 *Phys. Rev.* B **58** 8416
Chadi D J and Cohen M L 1973 *Phys. Rev.* B **8** 5747
Cunningham S L 1974 *Phys. Rev.* B **10** 4988
Dal Corso A 1996 *Quantum-Mechanical Ab-Initio Calculation of the Properties of Crystalline Materials (Springer Lecture Notes in Chemistry vol 67)* ed C Pisani (Berlin: Springer) p 77
Gilat G 1976 *Vibrational Properties of Solids (Methods in Computational Physics vol 15)* ed G Gilat (London: Academic) p 317
Lacks D and Rutledge G C 1994 *J. Phys. Chem.* **98** 1222
Monkhorst H J and Pack J D 1976 *Phys. Rev.* B **13** 5188
Taylor M B, Barrera G D, Allan N L and Barron T H K 1997 *Phys. Rev.* B **56** 14 380
Wallace D C 1972 *Thermodynamics of Crystals* (New York: Wiley)